Regioselectivity and Equilibrium Thermodynamics for Addition of Rh−OH to Olefins in Water

Xuefeng Fu, Shan Li, and Bradford B. Wayland*

Contribution from the Department of Chemistry, University of Pennsylvania, Philadelphia, Pennsylvania 19104-6323

Received December 8, 2005; E-mail: wayland@sas.upenn.edu

Abstract: Rhodium(III) tetra(*p*-sulfonato phenyl) porphyrin ((TSPP)Rh) aquo and hydroxo complexes react with a series of olefins in water to form β-hydroxyalkyl complexes. Addition reactions of (TSPP)Rh−OH to unactivated terminal alkenes invariably occur with both kinetic and thermodynamic preferences to place rhodium on the terminal carbon to form (TSPP)Rh−CH$_2$CH(OH)R complexes. Acrylic and styrenic olefins initially react to place rhodium on the terminal carbon to form Rh−CH$_2$CH(OH)X as the kinetically preferred isomer but subsequently proceed to an equilibrium distribution of regioisomers where Rh−CH(CH$_2$OH)X is the predominant thermodynamic product. Equilibrium constants for reactions of the diaquo rhodium(III) compound ([(TSPP)Rh^{III}(H$_2$O)$_2$]$^{-3}$) in water with a series of terminal olefins that form β-hydroxyalkyl complexes were directly evaluated and used in deriving thermodynamic values for addition of the Rh−OH unit to olefins. The $\Delta G°$ for reactions of the Rh−OH unit with olefins in water is approximately 3 kcal mol^{-1} less favorable than the comparable Rh−H reactions in water. Comparisons of the regioisomers and thermodynamics for addition reactions of olefins with Rh−H and Rh−OH units in water are presented and discussed.

Introduction

Exploring the scope and applications of organometallic transformations in water is a major current theme of transition metal catalysis research.[1−8] Our primary objectives in this area are to evaluate the reactivity patterns of rhodium porphyrins in water and to identify the dominant energy terms that govern the similarities and differences for analogous substrate reactions in organic and aqueous media.[6−8] Prior papers in this series have described reactions of tetra(*p*-sulfonato phenyl) porphyrin rhodium(III) ((TSPP)Rh^{III}) complexes in water with H$_2$/D$_2$[6] and the reactivity patterns of the rhodium hydride derivative ([(TSPP)Rh−D(D$_2$O)]$^{-4}$) in D$_2$O with olefins, aldehydes, and

CO that produce alkyl, α-hydroxyalkyl, and formyl complexes, respectively.[7,8] Comprehensive equilibrium thermodynamic studies for these rhodium porphyrin reactions in water provide a solid base for additional thermodynamic studies of rhodium-(III) porphyrin substrate reactions.[6,8]

Activation of olefins toward reactions with nucleophiles by coordination to metal centers is one of the most widely exploited synthetic organic methodologies,[9,10] and this approach continues to produce innovative developments in selective organic transformations.[11−16] Olefin binding and activation in water by transition metal species has a long history beginning in the early nineteenth century with Zeises' salt ([Cl$_3$Pt(CH$_2$=CH$_2$)]$^-$).[17] Palladium catalyzed oxidation of ethene to acetaldehyde by the "Wacker Reaction" and several closely related variants are

(1) (a) Cornils, B.; Kuntz, E. G. *Aqueous-Phase Organometallic Catalysis: Concept and Application*; Cornils, B., Herrmann, A. W., Eds.; Wiley-VCH: 1998; Chapter 6. (b) Lucey, D. W.; Helfer, D. S.; Atwood, J. D. *Organometallics* **2003**, *22*, 826−833. (c) Lucey, D. W.; Atwood, J. D. *Organometallics* **2002**, *21*, 2481−2490.
(2) (a) Stahl, S. S.; Labinger, J. A.; Bercaw, J. E. *Angew. Chem., Int. Ed.* **1998**, *37*, 2180−2192. (b) Stahl, S. S.; Labinger, J. A.; Bercaw, J. E. *J. Am. Chem. Soc.* **1996**, *118*, 5961−5976.
(3) (a) Lynn, D. M.; Grubbs, R. H. *J. Am. Chem. Soc.* **2001**, *123*, 3187−3193. (b) Lynn, D. M.; Mohr, B.; Grubbs, R. H.; Henling, L. M.; Day, M. W. *J. Am. Chem. Soc.* **2000**, *122*, 6601−6609.
(4) (a) Joo, F. *Acc. Chem. Res.* **2002**, *35*, 738−745. (b) Joo, F.; Kovacs, J.; Benyei, A. C.; Nadasdi, L.; Laurenczy, G. *Chem.—Eur. J.* **2001**, *7*, 193−199. (c) Joo, F.; Kovacs, J.; Benyei, A. C.; Katho, A. *Angew. Chem., Int. Ed.* **1998**, *37*, 969−970. (d) Csabai, P.; Joo, F. *Organometallics* **2004**, *23*, 5640−5643.
(5) (a) Kovacs, J.; Todd, T. D.; Reibenspies, J. H.; Joo, F.; Darensbourg, D. J. *Organometallics* **2000**, *19*, 3963−3969. (b) Darensbourg, D. J.; Joo, F.; Kannisto, M.; Katho, A.; Reibenspies, J. H.; Daigle, D. J. *Inorg. Chem.* **1994**, *33*, 200−208. (c) Darensbourg, D. J.; Joo, F.; Kannisto, M.; Katho, A.; Reibenspies, J. H. *Organometallics* **1992**, *11*, 1990−1993. (d) Parkins, A. W. In *Aqueous Organometallic Chemistry and Catalysis*; Horvath, I. T., Joo, F., Eds.; Kluwer Academic Publisher: Dordrecht, 1997; Vol. 11.
(6) Fu, X.; Wayland, B. B. *J. Am. Chem. Soc.* **2004**, *126*, 2623−2631.
(7) Fu, X.; Basickes, L.; Wayland, B. B. *Chem. Commun.* **2003**, 520−521.
(8) Fu, X.; Wayland, B. B. *J. Am. Chem. Soc.* **2005**, *127*, 16460−16467.

(9) McDaniel, K. F. In *Comprehensive Organometallic Chemistry II*; Abel, E. W., Stone, F. G. A., Wilkinson, G., Eds.; Elsevier Science Ltd.: Oxford, UK, 1995; Vol. 12, Chapter 7.
(10) Hegedus, L. S. Palladium in Organic Synthesis. In *Organometallics in Synthesis: a Manual*, 2nd ed.; Schlosser, M., Ed.; Wiley-Interscience: Chichester, UK, 1998.
(11) (a) Timokhin, V. I.; Anastasi, N. R.; Stahl, S. S. *J. Am. Chem. Soc.* **2003**, *125*, 12996−12997. (b) Brice, J. L.; Harang, J. E.; Timokhin, V. I.; Anastasi, N. R.; Stahl, S. S. *J. Am. Chem. Soc.* **2005**, *127*, 2868−2869. (c) Timokhin, V. I.; Stahl, S. S. *J. Am. Chem. Soc.* **2005**, *127*, 17888−17893.
(12) Pryadun, R.; Sukumaran, D.; Bogadi, R.; Atwood, J. D. *J. Am. Chem. Soc.* **2004**, *126*, 12414−12420.
(13) (a) Utsunomiya, M.; Hartwig, J. F. *J. Am. Chem. Soc.* **2004**, *126*, 2702−2703. (b) Takaya, J.; Hartwig, J. F. *J. Am. Chem. Soc.* **2005**, *127*, 5756−5757.
(14) Karshtedt, D.; Bell, A. T.; Tilley, T. D. *J. Am. Chem. Soc.* **2005**, *127*, 12640−12646.
(15) (a) Hong, S.; Marks, T. J. *Acc. Chem. Res.* **2004**, *37*, 673−686. (b) Ryu, J.-S.; Li, G. Y.; Marks, T. J. *J. Am. Chem. Soc.* **2003**, *125*, 12584−12605.
(16) (a) Chen, M. S.; White, M. C. *J. Am. Chem. Soc.* **2004**, *126*, 1346−1347. (b) Qian, H.; Widenhoefer, R. A. *Org. Lett.* **2005**, *7*, 2635−2638. (c) Brunet, J.-J.; Chu, N. C.; Diallo, O. *Organometallics* **2005**, *24*, 3104−3110.
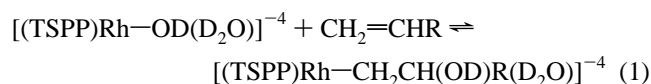(17) Zeise, W. C. *Annalen der Physik und Chemie* **1831**, *21*, 497−541.
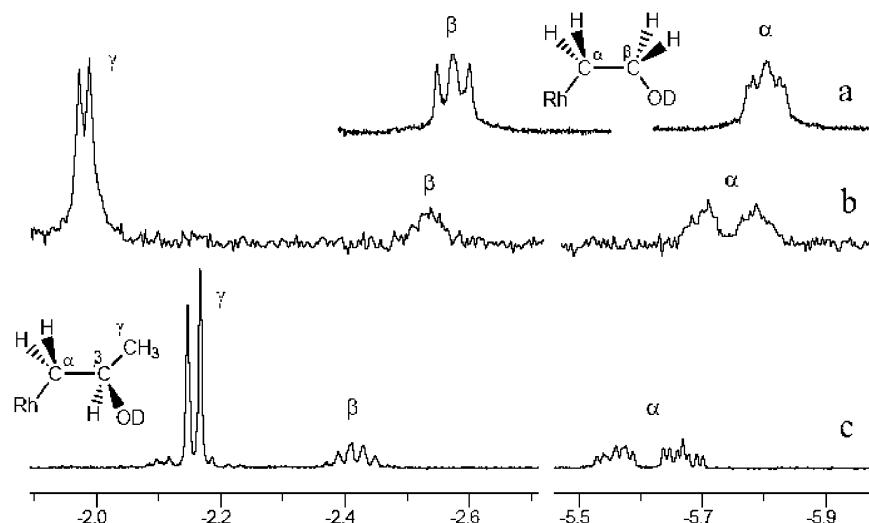
Figure 1. High field ^{1}H NMR (300 MHz) for (a) [(TSPP)Rh−CH$_2$CH$_2$(OD)(D$_2$O)]$^{-4}$ (**4**) in D$_2$O; (b) [(TSPP)Rh−CH$_2$CH(OD)CH$_3$(D$_2$O)]$^{-4}$ (**5**) in D$_2$O; (c) [(TSPP)Rh−CH$_2$CH(OD)CH$_3$(D$_2$O)]$^{-4}$ (**5**) in CD$_3$OD.
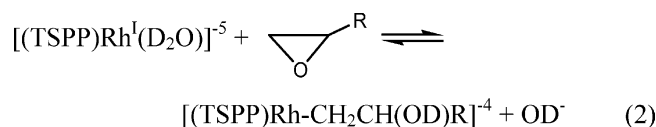
carried out in water and use reactions of coordinated alkenes with hydroxide and other nucleophiles as an essential step in the process.[17−19] This article reports on reactivity studies of (TSPP)Rh(III) complexes in water with olefins, and equilibrium thermodynamic measurements for the net addition of the rhodium hydroxide (Rh−OH) unit to C−C double bonds of terminal alkenes and activated olefins. Regioselectivity and thermodynamics are compared for addition reactions of Rh−OH and Rh−H with olefins in water.

Results and Discussion

Reactions of (TSPP)Rh^{III} Aquo/Hydroxo Species in D$_2$O with Terminal Alkene Hydrocarbons (CH$_2$=CHR, R = H, C$_n$H$_{2n+1}$): Rhodium(III) tetra(p-sulfonato phenyl) porphyrin hydrate complexes when dissolved in D$_2$O give solutions of the diaquo complex [(TSPP)Rh^{III}(D$_2$O)$_2$]$^{-3}$ (**1**) in fast equilibrium with mono and dihydroxo complexes ([(TSPP)Rh^{III}−OD(D$_2$O)]$^{-4}$ (**2**) and [(TSPP)Rh^{III}(OD)$_2$]$^{-5}$ (**3**)). Alkene hydrocarbons (CH$_2$=CHR) react with the monohydroxo rhodium (III) complex [(TSPP)Rh^{III}−OD(D$_2$O)]$^{-4}$ (**2**) in D$_2$O to form β-hydroxyalkyl organometallic derivatives (eq 1).

$$[(TSPP)Rh−OD(D_2O)]^{-4} + CH_2=CHR \rightleftharpoons$$
$$[(TSPP)Rh−CH_2CH(OD)R(D_2O)]^{-4} \quad (1)$$

Formation of β-hydroxyalkyl complexes in water is conveniently followed by the appearance of high field ^{1}H NMR resonances (0 to −6 ppm) associated with the organic groups bonded at the rhodium center that are shifted to high field by the porphyrin ring current. The ^{1}H−^{1}H and ^{103}Rh−^{1}H coupling patterns that are partially obscured by line broadening in water become clearly resolved by removing D$_2$O and redissolving in methanol (CD$_3$OD) (Figure 1). Assignments of the organometallic species formed by reactions of **2** with alkenes in D$_2$O using the ^{1}H NMR are confirmed by comparison with authentic samples prepared by the previously reported ring opening reactions of epoxides by rhodium(I) porphyrins (eq 2).[20,21] The ^{1}H NMR resonances
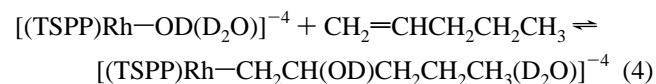
(18) (a) Smidt, J.; Hafner, W.; Jira, R.; Sedlmeier, J.; Sieber, R.; Rutlinger, R.; Kojer, H. *Angew. Chem.* **1959**, *71*, 176. (b) Phillips, F. C. *Am. Chem. J.* **1894**, *16*, 255.
(19) Takacs, J. M.; Jiang, X. *Current Organic Chemistry* **2003**, *7*, 369−396.

$$[(TSPP)Rh^I(D_2O)]^{-5} + \underset{O}{\overset{R}{\triangle}} \rightleftharpoons$$
$$[(TSPP)Rh-CH_2CH(OD)R]^{-4} + OD^- \quad (2)$$

centered at −5.76 and −2.52 ppm observed in the reaction of **2** with ethene (Figure 1a) are associated with the α-CH$_2$ and β-CH$_2$ groups, respectively, for the β-hydroxyethyl complex ([(TSPP)Rh−CH$_2$CH$_2$(OD)(D$_2$O)]$^{-4}$) (**4**) (eq 3). Compound **4** is observed to be identical to that produced by reaction of [(TSPP)Rh^I(D$_2$O)]$^{-5}$ with ethylene oxide.

$$[(TSPP)Rh−OD(D_2O)]^{-4} + CH_2=CH_2 \rightleftharpoons$$
$$[(TSPP)Rh−CH_2CH_2(OD)(D_2O)]^{-4} \quad (3)$$
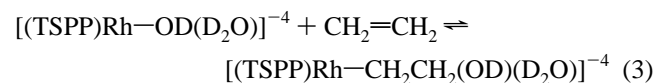
Propene and larger terminal alkene hydrocarbons react regioselectively with **2** to form β-hydroxyalkyl complexes where rhodium is attached to the terminal primary carbon ([(TSPP)-Rh−CH$_2$CH(OD)R(D$_2$O)]$^{-4}$) (Supporting Information).

The structure of the product from the reaction of **2** with propene in D$_2$O is confidently assigned to [(TSPP)Rh−CH$_2$-CH(OD)CH$_3$(D$_2$O)]$^{-4}$ (**5**) based on the ^{1}H NMR parameters (Figure 1) and confirmed by comparison with **5** produced by directed synthesis from reaction of propylene oxide with [(TSPP)Rh^I(D$_2$O)]$^{-5}$. Only a single isomer (**5**) is observed by ^{1}H NMR in water, and heating at 60 °C for extended periods of time does not result in ^{1}H NMR observable quantities of the alternate regioisomer ([(TSPP)Rh−CH(CH$_3$)CH$_2$(OD)(D$_2$O)]$^{-4}$). Similarly [(TSPP)Rh−CH$_2$CH(OD)CH$_2$CH$_2$CH$_3$(D$_2$O)]$^{-4}$ (**6**) is the exclusive isomer observed by ^{1}H NMR for the reaction of **2** with 1-pentene in D$_2$O (eq 4) (Supporting Information).

$$[(TSPP)Rh−OD(D_2O)]^{-4} + CH_2=CHCH_2CH_2CH_3 \rightleftharpoons$$
$$[(TSPP)Rh−CH_2CH(OD)CH_2CH_2CH_3(D_2O)]^{-4} \quad (4)$$

(20) Ogoshi, H.; Setsune, J.-I.; Yoshida, Z.-I. *J. Organomet. Chem.* **1980**, *185*, 95.
(21) (a) Wayland, B. B.; VanVoorhees, S. L.; Del Rossi, K. J. *J. Am. Chem. Soc.* **1987**, *109*, 6513−6515. (b) Han, Y.-Z.; Sanford, M. S.; England, M. D.; Groves, J. T. *Chem. Commun.* **2006**, 549−551.
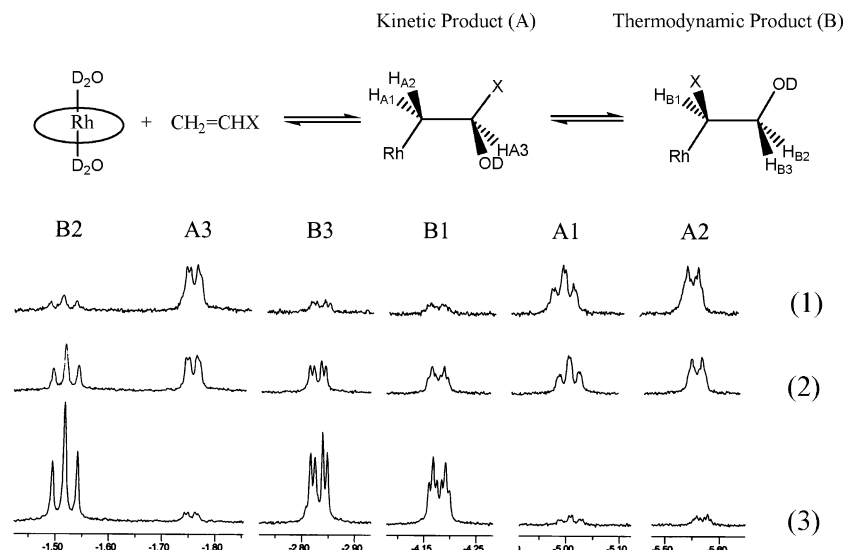
Figure 2. 500 MHz ^{1}H NMR in D$_2$O for reaction of [(TSPP)Rh−OD(D$_2$O)]$^{-4}$ with 4-styrene sulfonic acid sodium salt in D$_2$O ([D$^+$]$_{eq}$ ≈ 10^{-10} M) that forms [(TSPP)Rh−CH$_2$CH(OD)C$_6$H$_4$SO$_3$Na(D$_2$O)]$^{-4}$ (**8**) and (TSPP)Rh−CH(CH$_2$OD)C$_6$H$_4$SO$_3$Na(D$_2$O)]$^{-4}$ (**8′**) as a function of time. (1) t = 10 min, [**8**]/[**8′**] = 5; (2) t = 30 min, [**8**]/[**8′**] = 1; (3) t = 1.5 h, [**8**]/[**8′**] = 0.3.

Scheme 1. Pathways for Formation of Kinetic and Thermodynamic Products through Reactions of (TSPP)Rh(III) with Styrene in Water
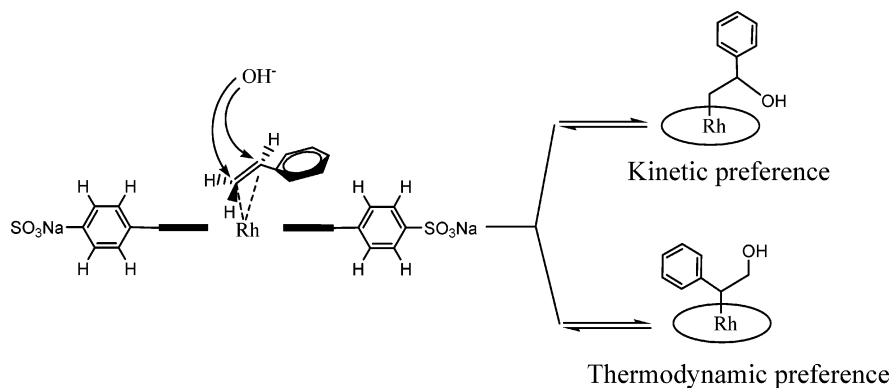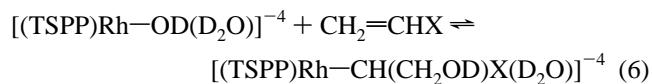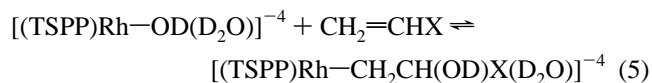

Undoubtedly, both regioisomers are formed by reactions of **2** with terminal alkenes (eq 1), but the isomer that places rhodium on the terminal primary carbon has both kinetic and thermodynamic preferences over the isomer where the rhodium porphyrin is attached to the more crowded secondary carbon. Addition of metal−nucleophile units to terminal alkenes usually places the metal at the terminal primary carbon and the nucleophile at the secondary carbon like that observed here for the Rh−OH unit, but Atwood has reported that amination of terminal alkenes using PtCl$_2$(PPh$_3$)(alkene) occurs with a kinetic preference for addition in the opposite direction which places the nucleophile on the primary carbon.[12]

Reactions of Rhodium(III) Porphyrin Species in D$_2$O with Activated Olefins (CH$_2$=CHX; X = C$_6$H$_5$, C$_6$H$_4$SO$_3$Na, CO$_2$H, and CO$_2$CH$_3$): Formation of products from reactions of (TSPP)Rh(III) species with activated olefins (CH$_2$=CHX); (X = C$_6$H$_5$, C$_6$H$_4$SO$_3$Na, CO$_2$H, and CO$_2$CH$_3$) were followed in D$_2$O solution by ^{1}H NMR. Regioisomers of the β-hydroxy-alkyl complexes ([Rh−CH$_2$CH(OD)X(D$_2$O)]$^{-4}$ and [Rh−CH(CH$_2$OD)X(D$_2$O)]$^{-4}$) that result from addition of the Rh−OD unit to olefins are easily distinguished in solution by the well separated and highly characteristic high field ^{1}H NMR peaks associated with the groups bonded to the rhodium porphyrin (Figures 1, 2).

Electrophilic olefins including styrene, 4-styrene sulfonic acid sodium salt, acrylic acid, and methyl acrylate (CH$_2$=CHC$_6$H$_5$, CH$_2$=CHC$_6$H$_4$SO$_3$Na, CH$_2$=CHCO$_2$H, and CH$_2$=CHCO$_2$CH$_3$) react rapidly with (TSPP)Rh^{III} species in D$_2$O to form [(TSPP)Rh−CH$_2$CH(OD)X(D$_2$O)]$^{-4}$ (X = C$_6$H$_5$, C$_6$H$_4$SO$_3$Na, CO$_2$H, and CO$_2$CH$_3$) (**7, 8, 9, 10**) as the kinetically preferred regioisomers (eq 5).

$$[(TSPP)Rh−OD(D_2O)]^{-4} + CH_2=CHX \rightleftharpoons$$
$$[(TSPP)Rh−CH_2CH(OD)X(D_2O)]^{-4} \quad (5)$$

$$[(TSPP)Rh−OD(D_2O)]^{-4} + CH_2=CHX \rightleftharpoons$$
$$[(TSPP)Rh−CH(CH_2OD)X(D_2O)]^{-4} \quad (6)$$

The initial kinetic products subsequently convert to an equilibrium distribution of regioisomers where the [(TSPP)Rh−CH(CH$_2$OD)X(D$_2$O)]$^{-4}$ complexes (X = C$_6$H$_5$, C$_6$H$_4$SO$_3$Na, CO$_2$H, and CO$_2$CH$_3$) (**7′, 8′, 9′, 10′**) are the thermodynamically preferred isomers (eq 6) (Scheme 1).

This reaction sequence is illustrated by the time evolution for the ^{1}H NMR of the products from reaction of **2** with a water soluble styrene derivative (CH$_2$=CHC$_6$H$_4$SO$_3$Na) shown in Figure 2. ^{1}H NMR taken immediately after mixing **2** with CH$_2$=CHC$_6$H$_4$SO$_3$Na shows a preponderance of the [(TSPP)-Rh−CH$_2$CH(OD)C$_6$H$_4$SO$_3$Na(D$_2$O)]$^{-4}$ (**8**) isomer which over

a period of hours converts to an equilibrium distribution of regioisomers where $[(TSPP)Rh-CH(CH_2OD)C_6H_4SO_3Na-(D_2O)]^{-4}$ (**8′**) is the predominant species (Figure 2).

Reactions of **2** with styrene and $[(TSPP)Rh^I(D_2O)]^{-5}$ with styrene oxide in D_2O produce $[(TSPP)Rh-CH_2CH(OD)C_6H_5-(D_2O)]^{-4}$ as the initial product which then isomerizes to the same equilibrium distribution of isomers. This pattern of kinetic and thermodynamic regioselectivities is observed for reaction of **2** with each of the styrenic and acrylic olefins studied. The kinetic and thermodynamic regioselectivities observed for the addition of the Rh—OH unit to activated olefins are unusual but parallel the observations recently reported by Stahl for the aminopalladation of styrene by $(NEt_3)_2PdCl_2$.[11] An electronic preference for placing the metal at the carbon center which best stabilizes negative charge has been identified as a significant contributing factor to the thermodynamic regioselectivity.[22]
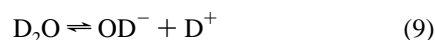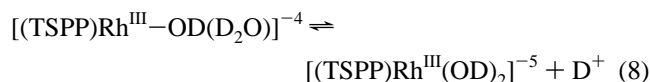
Reaction Pathways: The conventional mechanism to form β-hydroxyalkyl complexes from reactions of metal complexes with olefins involves the initial binding and activation of an olefin at the metal center followed by nucleophilic attack of water or hydroxide (Scheme 1). Although the concentrations of $(TSPP)Rh(III)$—olefin complexes in D_2O at the conditions used in this study were too small for direct observation by ^1H NMR, a rhodium(III) porphyrin ethene pi-complex has been observed to react reversibly with nucleophiles in benzene to form substituted alkyl complexes.[21] Olefin binding to the rhodium center activates both of the sp^2 carbon centers toward reaction with a nucleophile but gives a kinetic preference for hydroxide to approach the more congested carbon site. The bulky porphyrin binds with olefin substrates in the intermediate pi-complex in a manner that favors placing the rhodium porphyrin closer to the less sterically demanding olefin carbon center which preorganizes the transition state to form the Rh—$CH_2CH(OD)X$ regioisomer (Scheme 1). Alkene hydrocarbons ($CH_2=CHR$) have both kinetic and thermodynamic preferences for binding the rhodium through the terminal CH_2 group. Olefins where the terminal CH_2 is activated toward attack by a nucleophile have a kinetic preference for rhodium binding at the primary olefin carbon (Rh—$CH_2CH(OD)X$) but a thermodynamic preference for rhodium binding at the secondary carbon site (Rh—$CH(X)CH_2(OD)$). Facile reversibility for Rh—OD addition to olefins provides a route for the isomerization process.

Thermodynamics for Reactions of (TSPP)Rh^{III} Aquo/ Hydroxo Species with Olefins in Water: (TSPP)Rh^{III} Aquo and Hydroxo Complexes in Water: Evaluation of the equilibrium thermodynamic relationships between the (TSPP)Rh^{III} aquo/hydroxo complexes (**1**, **2**, **3**) in aqueous solution permits the deliberate quantitative tuning of the equilibrium distribution of species in D_2O by variation of the hydrogen ion concentration. This strategy is used to establish the set of conditions where equilibrium constants for olefin substrate reactions of rhodium-(III) porphyrin complexes can be measured directly by integration of the ^1H NMR for the (TSPP)Rh species in conjunction with measurements of the hydrogen ion concentration. Rhodium-(III) tetra(p-sulfonato phenyl) porphyrin hydrate complexes when dissolved in D_2O give solutions of a diaquo complex $[(TSPP)Rh^{III}(D_2O)_2]^{-3}$ (**1**) in fast equilibrium with mono and

(22) Harvey, J. N. *Organometallics* **2001**, *20*, 4887−4895.
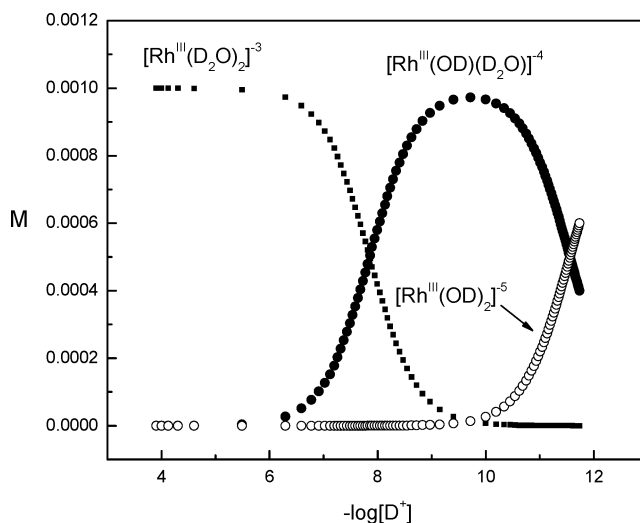
Figure 3. Equilibrium distributions of $[(TSPP)Rh^{III}(D_2O)_2]^{-3}$ (**1**), $[(TSPP)-Rh^{III}-OD(D_2O)]^{-4}$ (**2**), and $[(TSPP)Rh^{III}(OD)_2]^{-5}$ (**3**) as a function of the equilibrium hydrogen ion concentration ($[D^+]$) in D_2O at 298 K ($[(TSPP)-Rh^{III}]_T = 1.0 \times 10^{-3}$ M). (Calculated from measured K_7 and K_8.)

dihydroxo complexes $[(TSPP)Rh^{III}-OD(D_2O)]^{-4}$ (**2**) and $[(TSPP)Rh^{III}(OD)_2]^{-5}$ (**3**) (eqs 7, 8).

$$[(TSPP)Rh^{III}(D_2O)_2]^{-3} \rightleftharpoons$$
$$[(TSPP)Rh^{III}-OD(D_2O)]^{-4} + D^+ \quad (7)$$

$$[(TSPP)Rh^{III}-OD(D_2O)]^{-4} \rightleftharpoons$$
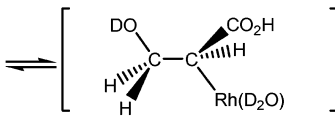$$[(TSPP)Rh^{III}(OD)_2]^{-5} + D^+ \quad (8)$$
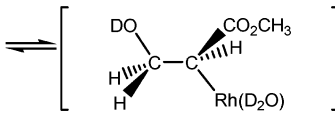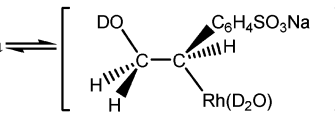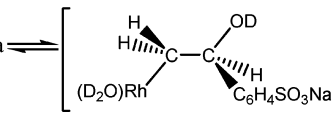
$$D_2O \rightleftharpoons OD^- + D^+ \quad (9)$$
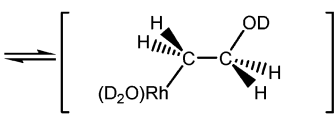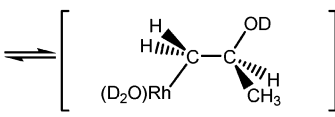
The mole fraction averaged ^1H NMR pyrrole resonance for **1**, **2**, and **3** as a function of the hydrogen ion concentration has been used to determine the acid dissociation constants (298 K) for coordinated D_2O in **1** ($K_7 = (1.4 \pm 0.2) \times 10^{-8}$) and **2** ($K_8 = (2.8 \pm 0.3) \times 10^{-12}$)[6] which are much larger than the acid dissociation constant for pure D_2O (K_3 (298 K) $= 2.44 \times 10^{-17}$). Changes in the distribution of **1**, **2**, and **3** in D_2O as a function of the equilibrium hydrogen ion concentration ($[D^+]$) are illustrated in Figure 3. The rhodium(III) diaquo complex (**1**) ($[(TSPP)Rh^{III}(D_2O)_2]^{-3}$) is the predominant species throughout the acidic range ($[D^+] > 3.7 \times 10^{-8}$ M) in D_2O. The monohydroxo complex **2** ($[(TSPP)Rh-OD(D_2O)]^{-4}$) constitutes more than 90% of the rhodium porphyrin species in solution when the $[D^+]$ is in the range of 1×10^{-9} to 3×10^{-11} M, and the dihydroxo complex (**3**) ($[(TSPP)Rh(OD)_2]^{-5}$) predominates when $[D^+]$ is less than 10^{-12} M (Figure 3).

Thermodynamics for Reactions of $[(TSPP)Rh-OD-(D_2O)]^{-4}$ with Terminal Olefins: In moderately basic D_2O ($[D^+] = 10^{-9}-10^{-10}$ M) the monohydroxo complex **2** predominates (Figure 3) and the olefin reactions with **1** ($[D^+] \approx 10^{-7}-10^{-5}$ M) effectively give quantitative conversion to β-hydroxyalkyl complexes. In acidic D_2O where the diaquo complex **1** is the predominant species, the alkene reactions are less thermodynamically favorable and achieve equilibrium distributions of **1** and organometallic species that are directly observable by ^1H NMR. Equilibrium constants for reactions of **1** with a series of olefins were evaluated from ^1H NMR of the solution species in conjunction with measurements of the hydrogen ion concentra-

Table 1. Directly Measured Equilibrium Constants (K_n) and $\Delta G°$ (kcal mol^{-1}) Values for the Reactions of [(TSPP)Rh^{III}(D$_2$O)$_2$]$^{-3}$ with Olefins in D$_2$O (T = 298 K)

[(TSPP)Rh^{III}(D$_2$O)$_2$]$^{-3}$ (1) Reactions	K_n	$\Delta G°_n$
10) **1** + CH$_2$=CH$_2$ ⇌ [(D$_2$O)Rh–CH$_2$–CH$_2$(OD)H]$^{-4}$ (**4**) + D$^+$	$K_{10} = 3.0(0.2) \times 10^{-4}$	4.8
11) **1** + CH$_2$=CHCH$_3$ ⇌ [(D$_2$O)Rh–CH$_2$–CH(OD)CH$_3$]$^{-4}$ (**5**) + D$^+$	$K_{11} = 1.1(0.5) \times 10^{-4}$	5.4
12) **1** + CH$_2$=CHCO$_2$H ⇌ [(DO)CH$_2$–CH(CO$_2$H)Rh(D$_2$O)]$^{-4}$ (**9'**) + D$^+$	$K_{12} = 4.0(0.9) \times 10^{-2}$	1.9
13) **1** + CH$_2$=CHCO$_2$CH$_3$ ⇌ [(DO)CH$_2$–CH(CO$_2$CH$_3$)Rh(D$_2$O)]$^{-4}$ (**10'**) + D$^+$	$K_{13} = 1.5(0.9) \times 10^{-2}$	2.5
14) **1** + CH$_2$=CHC$_6$H$_4$SO$_3$Na ⇌ [(DO)CH$_2$–CH(C$_6$H$_4$SO$_3$Na)Rh(D$_2$O)]$^{-4}$ (**8'**) + D$^+$	$K_{14} = 7.2(0.8) \times 10^{-5}$	5.7
15) **1** + CH$_2$=CHC$_6$H$_4$SO$_3$Na ⇌ [(D$_2$O)Rh–CH$_2$–CH(OD)C$_6$H$_4$SO$_3$Na]$^{-4}$ (**8**) + D$^+$	$K_{15} = 2.4(0.8) \times 10^{-5}$	6.3

tion ([D$^+$]). Experimentally measured equilibrium constants (298 K) in D$_2$O for reactions of the rhodium(III) diaquo complex **1** ([(TSPP)Rh^{III}(D$_2$O)$_2$]$^{-3}$) with olefin in D$_2$O to form β-hydroxyalkyl complexes are found in Table 1. Equilibrium constants and $\Delta G°$ values (298 K) are available for reactions of **1** with terminal alkene hydrocarbons that form Rh–CH$_2$CH(OD)R complexes, acrylates that produce Rh–CH(CO$_2$R)CH$_2$OD species and styrenic olefins that give observable equilibrium distributions of both regioisomers.

The distribution of the (TSPP)Rh^{III} species (**1**, **2**, **3**) in the ethene reaction to form [(TSPP)Rh–CH$_2$CH$_2$OD(D$_2$O)]$^{-4}$ (**4**) with the change in the equilibrium hydrogen ion concentration ([D$^+$]) is depicted in Figure 4. Effectively all of the (TSPP)-Rh^{III} species occur as the diaquo complex **1** when the [D$^+$] is 10^{-4} M or higher, but when the [D$^+$] is reduced to 1 × 10^{-6} M the β-hydroxyethyl organometallic complex ([(TSPP)Rh–CH$_2$CH$_2$(OD)(D$_2$O)]$^{-4}$ (**4**)) becomes approximately equal in concentration with that of **1** ([CH$_2$=CH$_2$] = 3.7 × 10^{-3} M) (Figure 4). The equilibrium constant for reaction 10 can be evaluated in the range of hydrogen ion concentration ([D$^+$] = 3 × 10^{-5} to 1 × 10^{-7} M) where both **1** and **4** have ^{1}H NMR observable concentrations. Figure 4 also illustrates that the monohydroxo complex **2** never builds up to high concentration because the reaction with ethene to form [(TSPP)Rh–CH$_2$CH$_2$-(OD)(D$_2$O)]$^{-4}$ (**4**) is thermodynamically highly favorable.
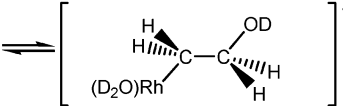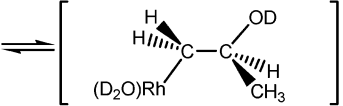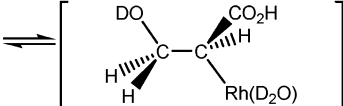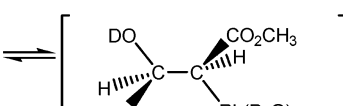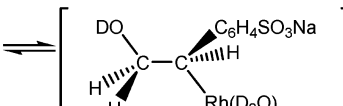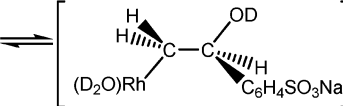
Equilibrium constants for reactions of the monohydroxo complex (**2**) with olefins are too large for direct measurement
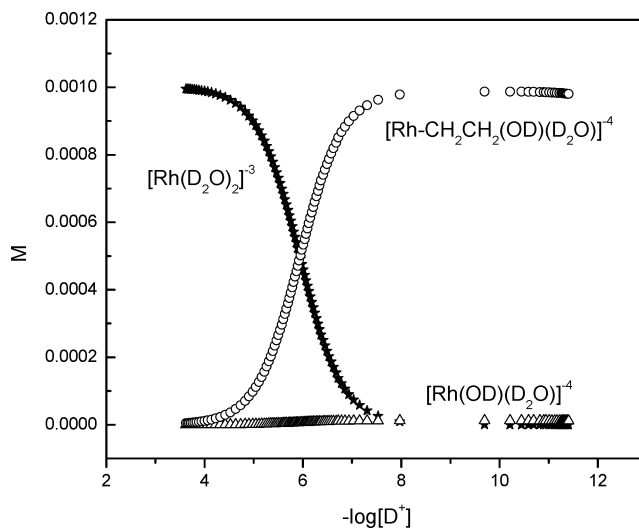
Figure 4. Change in the distribution of (TSPP)Rh^{III} species (**1**, **2**, **4**) from reaction of ethene as the equilibrium hydrogen ion concentration ([D$^+$]) is varied. (Calculated using K_7 and K_{10}.)

by ^{1}H NMR, but the K values can be obtained from thermodynamic cycles. This is illustrated by reaction of **2** with ethene (eq 3) which is given by the sum of reaction 10 with the reverse of reaction 7 (eq 7) which gives $K_3 = K_{10}/K_7 = 2.1(0.2) \times 10^4$ and $\Delta G_3° (298 K) = -5.9(0.1)$ kcal mol^{-1}.

Equilibrium constants and $\Delta G°$ values at 298 K for reactions of the monohydroxo complex [(TSPP)Rh–OD(D$_2$O)]$^{-4}$ (**2**) with the series of olefins are given in Table 2.

Table 2. Equilibrium Constants (K_n) and ΔG° (kcal mol^{-1}) Values for the Reactions of [(TSPP)Rh^{III}−OD(D$_2$O)]$^{-4}$ with Olefins in D$_2$O Derived from Table 1 (T = 298 K)

[(TSPP)Rh^{III}-OD(D$_2$O)]$^{-4}$ (**2**) Reactions	K_n	ΔG°_n
3) **2** + CH$_2$=CH$_2$ ⇌ (**4**)	$K_3 = K_{10}/K_1 = 2.1(0.2) \times 10^4$	−5.9
16) **2** + CH$_2$=CHCH$_3$ ⇌ (**5**)	$K_{16} = K_{11}/K_1 = 8.1(0.5) \times 10^3$	−5.3
17) **2** + CH$_2$=CHCO$_2$H ⇌ (**9'**)	$K_{17} = K_{12}/K_1 = 2.9(0.9) \times 10^6$	−8.8
18) **2** + CH$_2$=CHCO$_2$CH$_3$ ⇌ (**10'**)	$K_{18} = K_{13}/K_1 = 1.1(0.9) \times 10^6$	−8.2
19) **2** + CH$_2$=CHC$_6$H$_4$SO$_3$Na ⇌ (**8'**)	$K_{19} = K_{14}/K_1 = 5.1(0.8) \times 10^3$	−5.1
20) **2** + CH$_2$=CHC$_6$H$_4$SO$_3$Na ⇌ (**8**)	$K_{20} = K_{15}/K_1 = 1.7(0.9) \times 10^3$	−4.4

(10) [(TSPP)Rh^{III}(D$_2$O)$_2$]$^{-3}$ + CH$_2$=CH$_2$ ⇌ [(TSPP)Rh-CH$_2$CH$_2$(OD)(D$_2$O)]$^{-4}$ + D$^+$

(-7) [(TSPP)Rh-OD(D$_2$O)]$^{-4}$ + D$^+$ ⇌ [(TSPP)Rh^{III}(D$_2$O)$_2$]$^{-3}$

(3) [(TSPP)Rh-OD(D$_2$O)]$^{-4}$ + CH$_2$=CH$_2$ ⇌ [(TSPP)Rh-CH$_2$CH$_2$(OD)(D$_2$O)]$^{-4}$
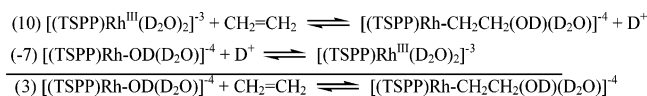
Comparison of Rh−OH and Rh−H Addition to Olefins in Water: Prior studies of Rh−H addition reactions of [(TSPP)-Rh−H(H$_2$O)]$^{-4}$ (**11**) with olefins in water permit comparisons of Rh−OH and Rh−H thermodynamics and regioselectivities for addition reactions with olefins.

Thermodynamics for addition of the Rh−OH and Rh−H units can be compared for terminal alkenes and styrene reactions that give the same regioselectivity (Table 3). The order of ΔG° values for the Rh−OH reactions is the same as that for Rh−H, and the difference between the ΔG° values for the Rh−H and Rh−OH addition reactions in water varies over only a small range (2.6−3.3 kcal mol^{-1}) (Table 3).

Terminal alkenes and acrylates give anti-Markovnikov addition of the Rh−H unit which places hydrogen at the secondary carbon to form the Rh−CH$_2$CH$_2$X (X = R, CO$_2$H, CO$_2$CH$_3$) regioisomer. Addition of the Rh−OH unit from [(TSPP)Rh−OH(H$_2$O)]$^{-4}$ to terminal olefins places rhodium on the primary CH$_2$ to form Rh−CH$_2$CH(OH)R which produces the same regioselectivity as the Rh−H reactions, but addition of the Rh−OH unit to acrylates (CH$_2$=CHCO$_2$R) places rhodium on the interior secondary carbon (Rh−CH(CH$_2$OH)CO$_2$R (**9'**, **10'**)) which is opposite to that observed for addition of Rh−H where rhodium bonds to the primary carbon (Rh−CH$_2$CH$_2$CO$_2$R). Adding the −OH group to an acrylate CH$_2$=CHCO$_2$R produces a rhodium bound substrate where intramolecular hydrogen bonding can occur. Improved intramolecular hydrogen bonding to form six-membered rings associated with **9'** and **10'** compared to the five-membered rings for **9** and **10** may be the thermodynamic factor that favors placing the −OH group on the terminal primary carbon (Figure 5).

The Rh−H reaction with styrene produces a mixture of regioisomers with a small preference for the Markovnikov product Rh−CH(C$_6$H$_5$)−CH$_2$D which contrasts with the exclusive anti-Markovnikov addition observed for the terminal alkenes and acrylates studied. Both Rh−H and Rh−OH add to styrene derivatives with a kinetic preference to place the rhodium at the least sterically demanding terminal carbon (Rh−CH$_2$CH-(Y)C$_6$H$_4$SO$_3$Na, Y = H, OH) and then proceed to form the isomer where rhodium is on the more sterically crowded interior carbon center (Rh−CH(CH$_2$Y)C$_6$H$_4$SO$_3$Na) as the favored thermodynamic product. Several precedents for this type of (por)RhCH$_2$CH$_2$Y rearrangement have been reported.[23] Spontaneous isomerization to a structure with increased unfavorable

Table 3. Comparison of $\Delta G°$ (kcal mol^{-1}) Values for Addition Reactions of Rh–OH and Rh–H to Olefins (298 K)

(TSPP)Rh-Y reactions (Y = H, OH)		$\Delta G°$	
		(Rh-OH)[a]	(Rh-H)[b]
$[Rh-Y]^{-4}$ + $CH_2=CH_2$ ⇌ [structure]		-5.9	-8.5
$[Rh-Y]^{-4}$ + $CH_2=CHC_6H_4SO_3Na$ ⇌ [structure]		-5.1	-8.2
$[Rh-Y]^{-4}$ + $CH_2=CHC_6H_4SO_3Na$ ⇌ [structure]		-4.4	-7.7

[a] Assuming that $\Delta G°$ values for addition reactions of Rh–OD and Rh–OH are equal. [b] Adjusted for isotope effect by reducing the $\Delta G°$ values measured for Rh–D addition by 0.4 kcal mol^{-1}.[8]

Rh-CH(CH$_2$OH)CO$_2$R   Rh-CH$_2$CH(OH)CO$_2$R
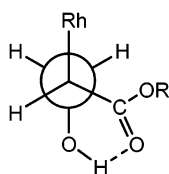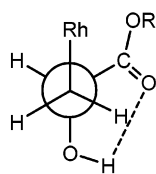
six-membered ring   five-membered ring

Figure 5. Intramolecular hydrogen bonding for β-hydroxy acrylates.

steric interactions implies that improved bonding interactions associated with placing both rhodium and phenyl on the same carbon center more than compensate for the unfavorable steric interactions. The polarity of the metal–organo bonds provides an electronic preference for the metal to bind the carbon center that forms the most stable carbanion.[22] The electron withdrawing phenyl group stabilizes the negative charge, and placing phenyl on the carbon center bonded to rhodium gives a favorable electronic energy term. The distribution of isomers is determined by the relative magnitudes of the competitive electronic and steric effects.

Conclusions: Olefins react with the Rh–OH unit of [(TSPP)-Rh–OD(D$_2$O)]$^{-4}$ (**2**) in water to produce β-hydroxyalkyl complexes. Reactions of **2** with terminal alkenes form Rh–CH$_2$CH(OH)R complexes with both kinetic and thermodynamic preferences to place rhodium on the terminal primary carbon. Activated electrophilic olefins react to form Rh–CH$_2$CH(OH)R complexes as the kinetically preferred isomer, and subsequently proceed to place rhodium at a secondary carbon center to form Rh–CH(CH$_2$OH)R complexes as the thermodynamically favored isomer. Reactions of Rh–OH and Rh–H fragments with terminal alkenes and styrene derivatives manifest the same regioselectivity. Acrylates (CH$_2$=CHCO$_2$R) react with Rh–OH and Rh–H with opposite regioselectivity which may result from the Rh–CH(CH$_2$OH)CO$_2$R isomer having the optimal intramolecular hydrogen bonding. The (TSPP)Rh–OH system provides

the first opportunity to determine equilibrium constants for addition reactions of a Rh–OH unit to olefins. The free energy changes for addition of the Rh–OH group with olefins are found to be about 3 kcal mol^{-1} less favorable than the parallel Rh–H reactions with olefins in water. Ligand structures and reaction media are illustrated as important factors in tuning the regioselectivity and thermodynamics for olefin substrate transformations.

Experimental Section

General Procedures: Proton NMR spectra were obtained on a Bruker AC-360 or AM-500 spectrometer interfaced to an Aspect 300 computer at ambient temperature. Chemical shifts were referenced to 3-trimethylsilyl-1-propanesulfonic acid sodium salt. Proton NMR spectra were used to identify solution species and to determine the distribution of species at equilibrium. The preparation of [(TSPP)Rh^{III}-(D$_2$O)$_2$]$^{-3}$ (**1**), [(TSPP)Rh–OD(D$_2$O)]$^{-4}$ (**2**), and [(TSPP)Rh^{III}(OD)$_2$]$^{-5}$ (**3**) were previously reported.[6-8]

Substrate reactions of (TSPP)Rh^{III} (**1, 2**) were carried out by mixing substrates in NMR tubes containing preformed samples of **1** and **2** (10^{-3} M) in D$_2$O at a defined hydrogen ion ([D$^+$]) concentration. Equilibrium constants were evaluated from the intensity integrations of ^{1}H NMR for each species in combination with D$^+$ concentration measurement and the solubility of the small organic substrates in water.

Measurements of [D$^+$] in D$_2$O. The glass electrode of a pH meter responds as efficiently to deuterium ions as it does with hydrogen ions, but the magnitude of the response is different.[24] Gary and co-workers have measured the activity of D$^+$ (α_D) from emf experiments. For identical solutions, the p(α_D) values differ from pH readings by a constant of 0.447 (p(α_D) – pH = 0.447).[25] The p(α_D) are measured in molal concentration. The conversion to molar units yields the relationship between the pH readings and the actual pD values as pD = pH$_{reading}$ + 0.41 (25 °C).

Equilibrium Constant Measurements for Substrate Reactions of (TSPP)Rh^{III} in D$_2$O. Proton NMR spectra were used to identify solution species and to determine the distribution of each species at equilibrium. The equilibrium constants were evaluated from the integrated intensity for the pyrrole porphyrin ^{1}H NMR resonance for each porphyrin species

(23) (a) Del Rossi, K. J.; Wayland, B. B. *J. Am. Chem. Soc.* **1985**, *107*, 7941–7944. (b) Mak, K. W.; Chan, K. S. *J. Am. Chem. Soc.* **1998**, *120*, 9686–9687. (c) Mak, K. W.; Xue, F.; Mak, T. C. W.; Chan, K. S. *J. Chem. Soc., Dalton Trans.* **1999**, 3333–3334.

(24) Glasoe, P. K.; Long, F. A. *J. Phys. Chem.* **1960**, *64*, 188–190.
(25) (a) Gary, R.; Bates, R. G.; Robinson, R. A. *J. Phys. Chem.* **1964**, *68*, 1186–1190. (b) Gary, R.; Bates, R. G.; Robinson, R. A. *J. Phys. Chem.* **1964**, *68*, 3806–3809. (c) Gary, R.; Bates, R. G.; Robinson, R. A. *J. Phys. Chem.* **1965**, *69*, 2750–2753.

in combination with D^+ concentration measurements and the solubility data of substrates in water.[26]

Reactions of [(TSPP)Rh$^{III}_{aq}$]$^{-3}$ with Ethene, Propene, and Pentene. [(TSPP)Rh−CH$_2$CH(OD)R-(D$_2$O)]$^{-4}$ was formed right after vacuum transfer of alkyl olefins (R = H, CH$_3$, and CH$_2$CH$_2$CH$_3$) into vacuum adapted NMR tubes containing D$_2$O solutions of [(TSPP)Rh−OD(D$_2$O)]$^{-4}$.

[(TSPP)Rh−CH$_2$CH$_2$(OD)(D$_2$O)]$^{-4}$ (**4**): ^{1}H NMR (360 MHz, D$_2$O) δ(ppm): 8.83 (s, 8H, pyrrole), 8.40 (d, 4H, *o*-phenyl, $J^1_{^1H-^1H}$ = 7.2 Hz), 8.29 (d, 4H, *o*-phenyl, $J^1_{^1H-^1H}$ = 7.2 Hz), 8.24 (d, 4H, *m*-phenyl, $J^1_{^1H-^1H}$ = 7.2 Hz), 8.20 (d, 4H, *m*-phenyl, $J^1_{^1H-^1H}$ = 7.2 Hz), −5.76 (br t, 2H(α)), −2.52, (t, 2 H(β), $J^1_{^1H-^1H}$ = 6 Hz).

[(TSPP)Rh−CH$_2$CH(OD)CH$_3$(D$_2$O)]$^{-4}$ (**5**): ^{1}H NMR (360 MHz, D$_2$O) δ(ppm): 8.83 (s, 8H, pyrrole), 8.40 (d, 4H, *o*-phenyl, $J^1_{^1H-^1H}$ = 7.2 Hz), 8.29 (d, 4H, *o*-phenyl, $J^1_{^1H-^1H}$ = 7.2 Hz), 8.24 (d, 4H, *m*-phenyl, $J^1_{^1H-^1H}$ = 7.2 Hz), 8.20(d, 4H, *m*-phenyl, $J^1_{^1H-^1H}$ = 7.2 Hz), −5.70(m, 1H$_A$ (α)), −5.76(m, 1H$_B$ (α)), −2.50 (m, 1H (β)), −1.97 (d, 3H(γ), 6 Hz).

[(TSPP)Rh−CH$_2$CH(OD)(CH$_2$)$_2$CH$_3$(D$_2$O)]$^{-4}$(**6**): ^{1}H NMR (360 MHz, D$_2$O) δ(ppm): 8.68 (8H, pyrrole), 8.50−8.10 (16H, phenyl), −5.96 (m, 1H$_A$(α)), −5.75 (m, 1H$_B$(α)), −3.02 (m, 1H(β)), −2.66 (m, 1H$_A$(γ)), −1.77 (m, 1H$_B$(γ)), −0.72 (m, 2H(δ)), −0.31 (t, 3H(ϵ)).

Reactions of [(TSPP)Rh$^{III}_{aq}$]$^{-3}$ with Styrene, 4-Styrenesulfonic Acid Sodium Salt, Acrylic Acid, and Methyl Acrylate. Mixing aqueous solutions of **2** with styrene, 4-styrenesulfonic acid sodium salt, acrylate acid, and methyl acrylate initially produce [(TSPP)Rh−CH$_2$-CH(OD)C$_6$H$_5$(D$_2$O)]$^{-4}$ (**7**), [(TSPP)Rh−CH$_2$CH(OD)C$_6$H$_4$SO$_3$Na-(D$_2$O)]$^{-4}$ (**8**), [(TSPP)Rh−CH$_2$CH(OD)CO$_2$H]$^{-4}$ (**9**), [(TSPP)Rh−CH$_2$CH(OD)CO$_2$CH$_3$(D$_2$O)]$^{-4}$ (**10**) as the kinetically preferred isomers which subsequently rearrange to produce [(TSPP)Rh−CH(C$_6$H$_5$)CH$_2$-(OD)(D$_2$O)]$^{-4}$ (**7′**), [(TSPP)Rh−CH(C$_6$H$_4$SO$_3$Na)CH$_2$(OD)(D$_2$O)]$^{-4}$ (**8′**), [(TSPP)Rh−CH(CO$_2$H)CH$_2$(OD)(D$_2$O)]$^{-4}$ (**9′**), and [(TSPP)Rh−CH(CO$_2$CH$_3$)CH$_2$(OD)(D$_2$O)]$^{-4}$ (**10′**) as the thermodynamically preferred products.

[(TSPP)Rh−CH$_2$CH(OD)CO$_2$H(D$_2$O)]$^{-4}$: ^{1}H NMR (500 MHz, D$_2$O) δ(ppm): 8.86 (s, 8H, pyrrole), 8.37, 8.34, 8.21, 8.20 (4d, 16H, phenyl,

$J^1_{^1H-^1H}$ = 8.3 Hz), −1.98 (t, 1H, CH$_2$X, $^3J^1_{^1H-^1H}$ = 11.4 Hz, $^2J^1_{^1H-^1H}$ = 11.8 Hz), −3.12 (d of d, 1H, CH$_2$X, $^3J^1_{^1H-^1H}$ = 3.6 Hz, $^2J^1_{^1H-^1H}$ = 11.8 Hz), −4.81 (d of t, 1H, C(CO$_2$D)**H**, $^3J^1_{^1H-^1H}$ = 11.4, $^3J^1_{^1H-^1H}$ = 3.6 Hz, $J^{103}_{Rh-^1H}$ = 4.0 Hz).

[(TSPP)Rh−CH(CO$_2$H)CH$_2$(OD)(D$_2$O)]$^{-4}$: ^{1}H NMR (500 MHz, D$_2$O) δ(ppm): 8.86 (s, 8H, pyrrole), 8.37, 8.34, 8.21, 8.20 (4d, 16H, phenyl, J_{1H-1H} = 8.3 Hz), −1.79 (t, 1H, **CH**(CO$_2$D)(OD), $^3J^1_{^1H-^1H}$ = 7.4 Hz, $^2J^1_{^1H-^1H}$ = 7.1 Hz), −3.7 (m, 1H, **CH**$_2$), −3.9 (m, 1H, **CH**$_2$).

[(TSPP)Rh−CH(CO$_2$CH$_3$)CH$_2$(OD)(D$_2$O)]$^{-4}$: ^{1}H NMR (250 MHz, D$_2$O) δ(ppm): 8.90 (s, 8H, pyrrole), 8.47−8.20 (m, 16H, phenyl), 1.86 (s, 1H, OCH$_3$), −1.79 (t, 1H, **CH**(CO$_2$CH$_3$), $^3J^1_{^1H-^1H}$ = 11.2 Hz), −3.06 (d of d, 1H, **CH**$_2$, $^3J^1_{^1H-^1H}$ = 4.1 Hz, $^2J^1_{^1H-^1H}$ = 11.2 Hz), −4.9 (d of t, 1H, **CH**$_2$, $^3J^1_{^1H-^1H}$ = 4.1 Hz, $^2J^1_{^1H-^1H}$ = 11.2 Hz).

[(TSPP)Rh−CH$_2$CH(OD)C$_6$H$_4$SO$_3$Na(D$_2$O)]$^{-4}$: ^{1}H NMR (360 MHz, D$_2$O) δ(ppm) 8.80 (s, 8H, pyrrole), 8.46, 8.34, 8.27, 8.20 (4d, 16H, phenyl, $J^1_{^1H-^1H}$ = 8.0 Hz), −1.97 (d, 1H, **CH**$_2$, $^2J^1_{^1H-^1H}$ = 10 Hz) −5.17 (t, 1H, **CH**$_2$, $^2J^1_{^1H-^1H}$ = 10 Hz), −5.65 (d, 1H, CH, $J^1_{^1H-^1H}$ = 5 Hz).

[(TSPP)Rh−CH(C$_6$H$_4$SO$_3$Na)CH$_2$OD(D$_2$O)]$^{-4}$: ^{1}H NMR (360 MHz, D$_2$O) δ(ppm) 8.80 (s, 8H, pyrrole), 8.46, 8.34, 8.27, 8.20 (4d, 16H, phenyl, $J^1_{^1H-^1H}$ = 8.0 Hz), −1.55 (t, 1H, **CH**$_2$, $^2J^1_{^1H-^1H}$ = 11.5 Hz) −2.87 (d of d, 1H, **CH**$_2$, $^3J^1_{^1H-^1H}$ = 4.2 Hz, $^2J^1_{^1H-^1H}$ = 11.5 Hz), −4.23 (d of t, 1H, CH, $J^1_{^1H-^1H}$ = 4.2 Hz, $J^{103}_{Rh-^1H}$ = 1.5 Hz).

[(TSPP)Rh−CH$_2$CH(OD)C$_6$H$_5$(D$_2$O)]$^{-4}$: ^{1}H NMR (360 MHz, D$_2$O) δ(ppm) 8.80 (s, 8H, pyrrole), 8.46−8.20 (m, 16H, phenyl), −1.95 (b, 1H, **CH**$_2$), −5.15 (b, 1H, **CH**$_2$), −5.65 (b, 1H, CH).

[(TSPP)Rh−CH(C$_6$H$_5$)CH$_2$OD(D$_2$O)]$^{-4}$: ^{1}H NMR (360 MHz, D$_2$O) δ(ppm) 8.80 (s, 8H, pyrrole), 8.46−8.20 (b, 16H, phenyl), −1.67 (b, 1H, **CH**$_2$), −2.97 (b, 1H, **CH**$_2$), −4.30 (b, 1H, CH).

Supporting Information Available: Experimental details regarding the preparation and ^{1}H NMR spectra for compounds **1**−**10**; equilibrium constant measurements for substrate reactions of (TSPP)Rh(III) in D$_2$O; estimation of the bond dissociation free energy and bond dissociation enthalpy for the Rh−OH unit in water and benzene.

JA0583416

(26) Fog, P. G. T.; Gerrard, W. *Solubility of Gases in Liquids: A Critical Evaluation of Gas/Liquid Systems in Theory and Practice*; Wiley: Chichester, NY, 1991.